Continuous Onshore Seismic Reservoir Monitoring of Thermal EOR in the Netherlands

Julien Cotton, Laurene Michou, Eric Forgues*, CGG; Kees Hornman, Shell Global solutions international

A continuous reservoir monitoring system was installed for Shell on the Schoonebeek medium heavy-oil onshore field situated in the north-east of the Netherlands, in the context of re-development of oil production by Gravity Assisted Steam Flood. The challenge was to continuously monitor, with seismic reflection, the lateral and vertical expansion of the steam chest injected in the reservoir during production for a period of over more than a year.

The main problems encountered with onshore time-lapse acquisition are caused by near-surface variations between base and monitor surveys which affect the seismic signal coming from the reservoir. Here, a set of permanent shallow buried sources and sensors were installed below the weathering layer to both mitigate the near surface variations and minimize the environmental footprint.

The Schoonebeek field has a STOIIP of 1 bln bbls. The medium heavy-oil reservoir is about 20 meters thick and located at a depth of 650 meters, with an average porosity of 30%. Between 1948 and 1996, the oil (160 cP at 40°C, 25 API, 19% wax) was produced with several small-scale thermal EOR pilots with vertical wells. Today the oil is produced by Gravity Assisted Steam Drive.

A permanent seismic system including a 2D and 3D phase was installed in 2010 to monitor the reservoir's behavior during the steam injection (Figure 1). The monitoring period lasted two years. During this time, we tracked the propagation of the steam plume injected into a horizontal well located between two horizontal producer wells in order to understand the 4D behavior of the steam and possibly update the dynamic production model.

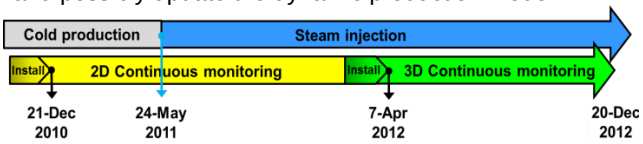

Figure 1: Permanent seismic monitoring time schedule covering the transition period between cold production and steam injection. Black triangles represent the system's installation period.

Gravity Assisted Steam Drive

Reservoir engineers are interested in knowing how the steam spreads from the injector to the neighboring producers. The pump rate could be adjusted in order to optimize reservoir production.

The steam, injected at low pressure, is expected to rise to the top of the reservoir, then to spread horizontally and finally to condense. Hot water will descend through the reservoir, heating the oil and improving its mobility.

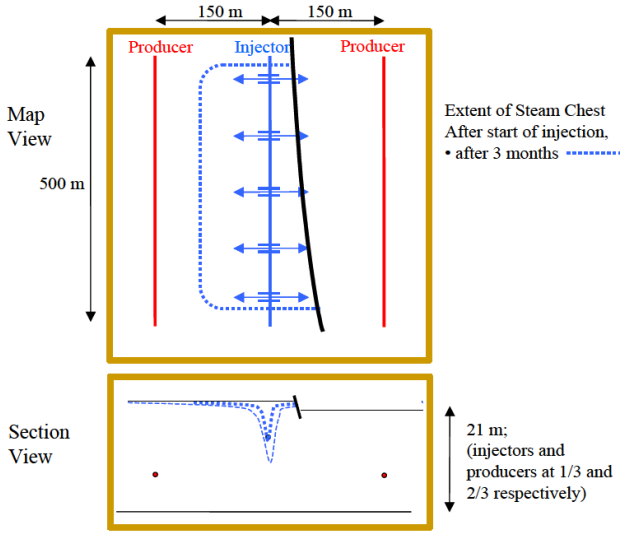

Figure 2: asymmetric expansions of the steam chest due to the small fault throw

According to Hornman et al., 2012, a 3-m sub-seismic fault may delay steam expansion by three years as shown in Figure 2 with an example of asymmetrical steam chest development.

A feasibility study was conducted by modeling the acoustic response of the pressure during cold production and steam injection. During the early steam injection phase, pressure, temperature and steam zone thickness should change, but in a different way:

1) The pressure changes should propagate quickly over the reservoir and will be nearly the same over the vertical dimension of the reservoir.
2) The steam zone should initially be thin and should propagate horizontally along the top of the reservoir.
3) The associated temperature increase should first be near the top of the reservoir and then increase vertically below the steam zone.

2D & 3D Seismic Monitoring

A permanent buried monitoring installation ensures excellent seismic repeatability, as well as having a minimum impact on surrounding farming activities and on the environment (Figure 3). First, in December 2010, a 2D pilot survey was carried out (see Cotton et al. 2012 for a detailed description). Second, in April 2012, the permanent seismic acquisition geometry was extended to 3D.

Figure 3: Aerial photos of the monitoring area. Top: trenches during installation. Bottom: four months later during continuous monitoring.

The 3D system consists of 36 piezoelectric mini-vibrators (Figure 4) placed into cemented boreholes at a depth of 25 meters. The signal was recorded by a set of five lines each of them, composed of 69 dual-depth hydrophones buried at 6 and 9 meters. As illustrated in Figure 5, the equipment was located above one horizontal injector and two horizontal producers. There were also two deviated observation wells measuring the temperature and pressure at two locations inside the reservoir. The sources vibrated simultaneously and continuously during the two year acquisition period, thanks to a patented technique (IFP, GDF, CGG, US patent 6714867-B2) of mono-frequency emissions covering a 4-186 Hz band over six hours.

Figure 4: A SeisMovie™ piezoelectric source to be cemented down hole.

The 3D acquisition covered a subsurface imaging area of 800 by 120 meters.
A daily summed shot point is shown in Figure 6. The zero-offset reservoir reflection arrives at 625 milliseconds. The energetic S-wave cone generated by the source hides the near offsets and is consequently muted. As a result, at the reservoir level, the contributing offset extends only from 250 to 800 meters and the stacking fold ranks from 4 to 8 in the useful part of the spread covering the injection and the production wells. This very low fold is counter-balanced by favorable data quality and high repeatability provided by the buried sources and receivers under the weathering layer.

Unfortunately, there are three other types of unwanted waves interfering with the reservoir reflections: i) the S-P wave converted at the surface, ii) the source ghosts iii) the receiver ghosts. Minimization of these unwanted waves is necessary to ensure an accurate recovery of the seismic monitoring results.

The processing sequence described in Cotton and Forgues, 2012 was automatically executed on a daily basis to provide migrated seismic cubes and 4D attributes (travel time and amplitude variations). The processing has two main objectives: first, the mitigation of surface-reflected waves interfering with the reflections around the reservoir (ghost and near-surface converted waves); second, the focusing of the diffractions in order to map amplitude changes in the reservoir. The processing workflow consists of:

1. receiver ghost reduction by dual-depth hydrophone combinations,
2. source ghost separation in the calendar domain,
3. S-P converted wave mitigation by separation in the calendar domain (Bianchi et al., 2004), plus a high-resolution 3D radon filter to remove residual linear waves,
4. weekly sliding median filter in the calendar domain to remove remaining industrial noise,
5. post-stack migration with a constant velocity to focus the diffracted events,
6. Daily computation of 4D attributes: amplitude and travel time variations are obtained using cross-correlation with a reference.

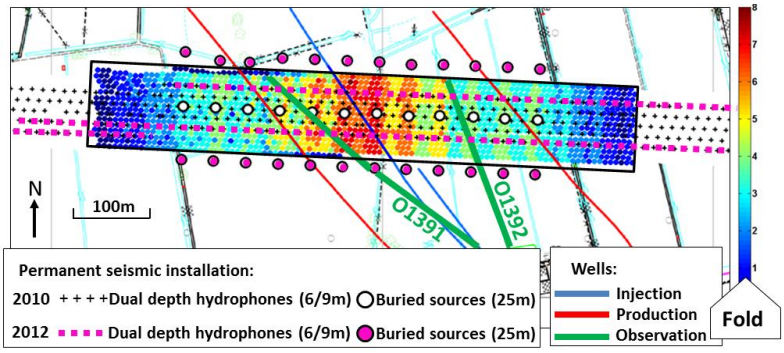

Figure 5: Map showing the equipment procured for both the initial 2010 2D survey and added in 2012 to enable 3D monitoring. The colored dots represent the imaging bins with the associated fold.

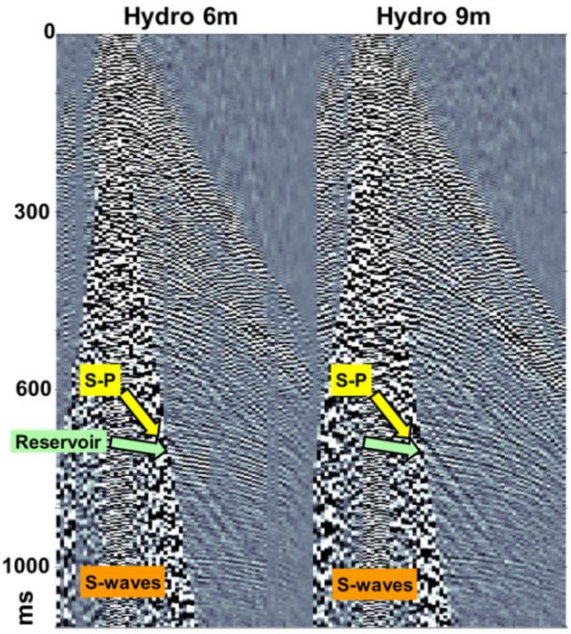

Figure 6: Typical shot point recorded daily for one buried source and a line of dual-depth hydrophones buried at 6 and 9 meters depths.

The repeatability improvement brought about by the processing can be represented as the reduction in both amplitude and travel time variations above the reservoir, as shown in Figure 7 (a perfect repeatability would produce dots at the origin of both axes). Both, the source and the receiver de-ghosting dramatically improve the repeatability. The de-ghosting clearly enhances the repeatability but it does not particularly improve the general visual aspect of the stack section shown in Figure 8. On the contrary, the migration only slightly improves the repeatability, but enhances the general image quality, by reducing the noise level and by focusing the signal.

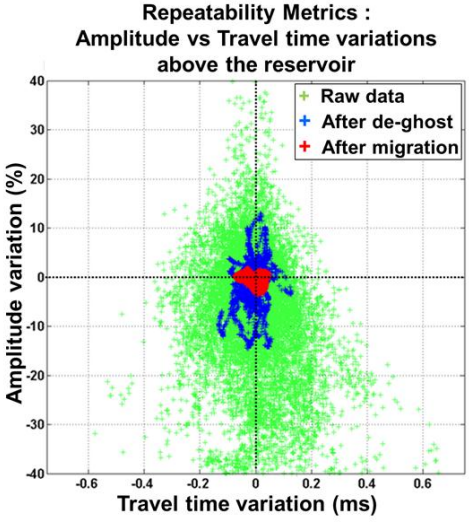

Figure 7: Cross plot of amplitude and travel time variations computed by cross-correlation above the reservoir, in the time windows shown in Figure 8

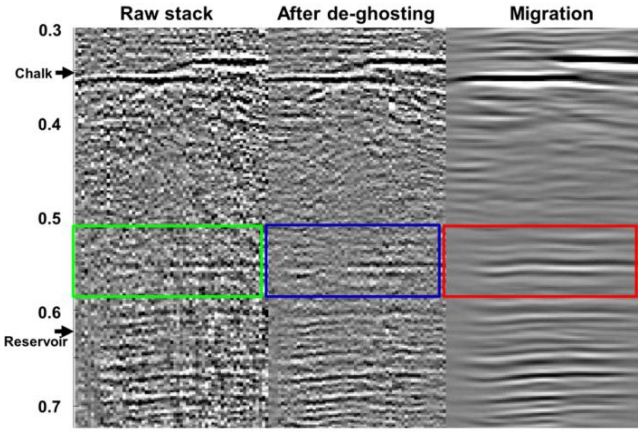

Figure 8: Seismic stack section from the 3D cube, for the raw data and after the two main processing stages i) de-ghosting and, ii) post-stack migration. The colored time windows above the reservoir are used to compute the cross plots in Figure 7

4D Monitoring Results

In Figure 9, the difference between two migrated sections crossing the wells at two different dates is a way of evalyating the seismic signal variation within the reservoir. We clearly observe a seismic 4D effect in the vicinity of the injector. The difference (multiplied by 5) is represented here at the early stage of the injection during the 2D phase (one month before the start of the injection on the 24th of April 2011 and one month after on the 24th of June 2011).

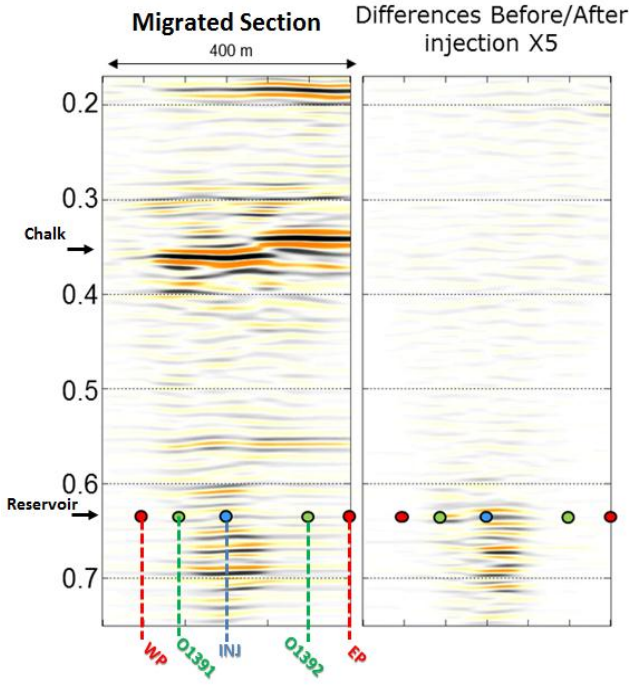

Figure 9: Left: Stack section with well locations (extracted from the seismic from the 2D phase). Right: differences multiplied by 5 between sections one month before and one month after the start of injection

For both the 2D and 3D seismic monitoring, the daily 4D attributes are obtained using a trace-by-trace cross-correlation with a reference dataset. The lengths of the correlation windows are 100 and 20 milliseconds for the travel times and the amplitudes respectively.
The 4D attributes are then compared to actual well information. For the 2D phase the same comparison has been described in Cotton et al., 2012.
At the injector, the seismic attributes are compared to the injection steam rate (Figure 10). The steam injection started on May 9th, 2011, and the full injection started around May 24th, 2011. This graphical comparison highlights that the steam injection and interruptions are detected almost instantaneously on the time shift curve (red line) and with some delay on the amplitude curve (green line). There is virtually no change above the reservoir (light lines). The time shifts occur very rapidly, following the steam injection rate. These travel time variations can be interpreted as essentially pressure change effects. Near the injector, three months after the start of steam injection, the maximum observed cumulative variation in amplitude and time shift are 10% and 0.4 milliseconds respectively. During the same period, the average calculated daily time shift variations are about 6 microseconds and the daily amplitude variations are about 0.1%.
In Figure 11, we see a good correlation between the travel time variations and the pressure measured at the two observation wells. Between April and December 2011, pressure effects were detected on both observation wells O1391 and O1392, each located 80 and 160 meters from the injector.

Between April and December 2012, almost no pressure effects were detected at the observation wells, while the steam injection rate and the travel time variation at the injector were both rising (Figure 10).

The 3D monitoring system is required to understand and map the complex path of the steam propagation following the injection period. To visualize the daily evolution of the amplitude variations, a 4D movie was produced. Figure 12 shows four maps at different dates. The travel time variations were measured below the reservoir at 675 milliseconds and the amplitude variations were measured in the reservoir at 625 milliseconds. On the amplitude variation maps (left column), we see that the steam propagates from the injector well (blue) to the western production well (red) passing north of the western observation well O1391 (green). No significant variations are observed on the east side of the injector well. This suggests that the small fault situated inside the reservoir and between the injector and the eastern producer shown in Figures 13 and 14 reduces the steam propagation.

Figure 13 shows snap shots of the 4D movie computed during the injection. The 3D yellow “blob” is the 7% iso amplitude variation compared to May 2012. It represents the spatial and calendar amplitude spreading due to steam injection.

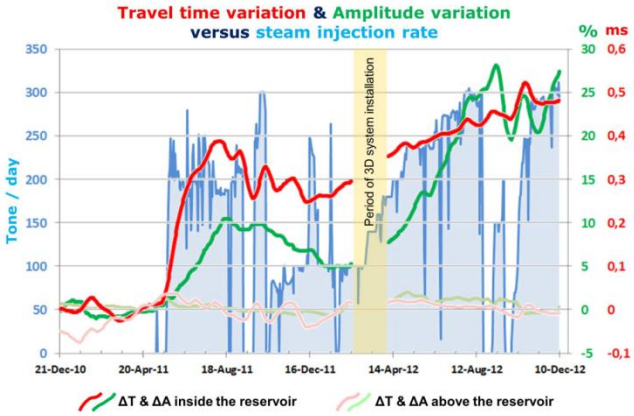

Figure 10: At the injection well, the steam injection rate (blue) is correlated with the seismic travel time shift (red) and amplitude (green) measured at CDP #51 below the reservoir. Above the reservoir, the time shift and the amplitude variations (light red and light green) are very stable around zero.

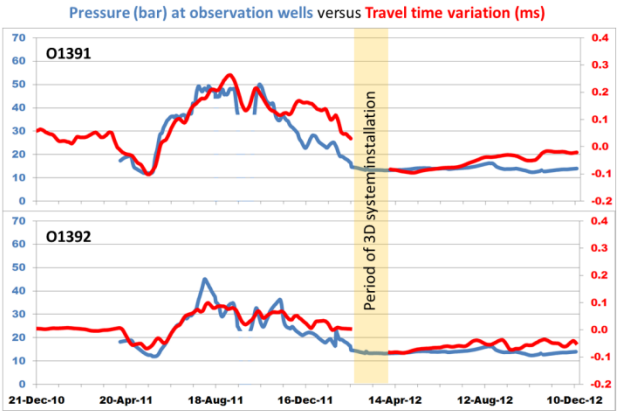

Figure 11: Comparison between travel time variations and pressure measured at both observation wells 1391 on the east (Top) and O1392 on the west (Bottom)

The amplitude variations obtained by cross-correlation give a cumulative effect of the steam over the whole reservoir thickness but do not allow us to distinguish the 4D effects between the top and the base of the reservoir. To investigate what happens inside the reservoir, a 4D acoustic inversion was carried out on a monthly basis. The stratigraphic inversion allows a better vertical resolution as shown in Figure 15 where panel 15b shows a 2ms layer resolution with a total 4ms impedance variation at the top of the reservoir while in panel 15f the amplitude variation computed with cross-correlation on a sliding 20ms time window is less focused.
Although the quantification of 4D effects in terms of P-impedance variations (-8%) was in agreement with the Petro Elastic Model, the very low seismic fold with a limited offset range restricted the 4D inversion to estimation of the acoustic P-impedance variations only. But the P-impedance variations alone are not sufficient to understand the complex rock physics phenomena that occur during the steam propagation.

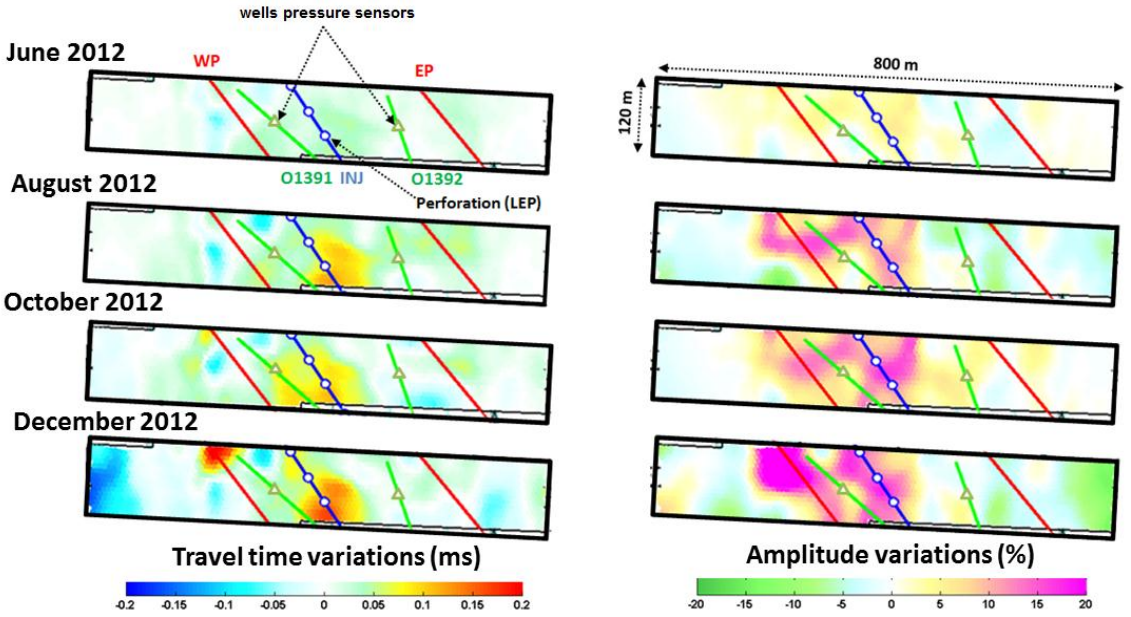

Figure 12: Travel time variations below the reservoir (Left) and amplitude variations in the reservoir (Right) at different dates. The east part of the reservoir is clearly not swept by the steam.

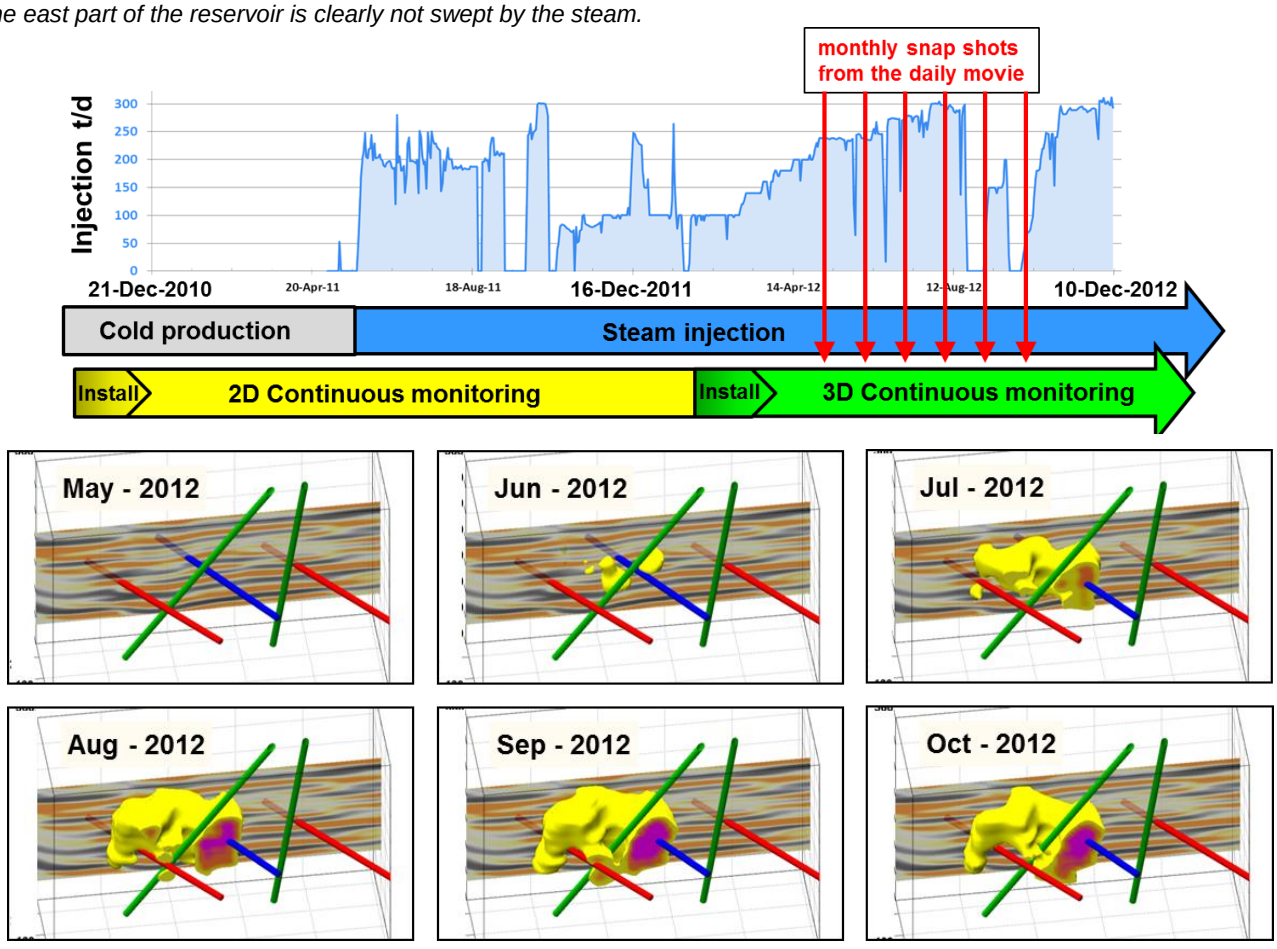

Figure 13: The 3D volumes of the iso 7% amplitude variations (yellow) shows the evolution of the steam chamber in the reservoir at different times of the injection (represented in red arrows on the injection curve). The steam propagation is delayed by a small discontinuity between the injector and the eastern producer. This small discontinuity is visible on figure 14 on the bottom reservoir horizon (grey surface) picked on the conventional 2005 3D seismic.

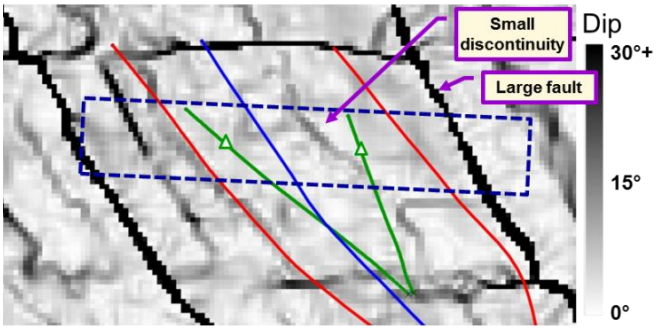

Figure 14: Map of the dips at the base of the reservoir computed using an existing 3D surface dataset acquired in 2005 (Courtesy of NAM). The permanent monitoring area is represented by the dashed rectangle. A small fault exists between the injector in blue and the eastern producer in red.

The next step would be quantitative validation of the P-impedance variations and interpretation of their evolution in terms of fluid or temperature variations as they do not occur in the same way over period of time measured. To do so, we plan to use additional constraints coming from the Petro-Elastic-Model and take advantage of the high resolution in the calendar domain.

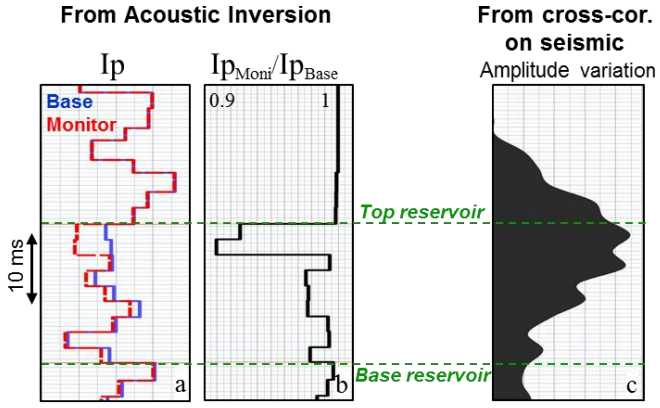

Figure 15: 4D inversion results at the injection well: (a) P impedance for base (blue), monitor (red), (b) monitor over base impedance ratio, (c) and

Conclusions

The very high sensitivity of our buried acquisition system allowed the tracking/monitoring of very small variations in the reservoir's physical properties in both the spatial and calendar domains.

The 4D reservoir attributes obtained from seismic monitoring fit the measurements made at observation, production and injector wells (pressure, temperature and oil/water production).

A "daily 4D movie" of the changes in reservoir properties allowed the proposition of a scenario which explains the unexpected behavior of the production and confirms that the steam does not follow the expected path to the producer wells but rather takes a more complicated 3D path within the reservoir.

The precision and stability of our permanent and continuous buried acquisition system allowed us to detect both small travel time and amplitude variations over a period of two years. The accuracy of these values is confirmed by measurements made at the observation wells.

The deployment of the 3D survey enabled us to investigate the complex path taken by the steam from the injector to the producer, providing valuable information to build more accurate dynamic models for better reservoir management decisions.

The benefit of the 4D acoustic inversion trial conducted on this dataset is the vertical resolution that is used to differentiate Ip variations between the top and base of the reservoir.

These good results encourage us to pursue the analysis of this inspiring dataset. On the one hand, an experiment using a pre-stack time migration to provide angle stacks for the inversion process will be attempted. On the other, we plan to differentiate pressure, saturation and temperature effects using additional constraints from the Petro-Elastic-Model and taking advantage of the high resolution in the calendar domain.

Acknowledgements

We would like to thank Shell Global Solutions International and NAM for their kind permission to present this work. We would like to thank Julien Meunier, Yves Lafet and Thierry Coleou for the fruitful discussion that we have together.

References

T. Bianchi, E. Forgues, J. Meunier, F. Huguet, and J. Bruneau, 2004, Acquisition and processing challenges in continuous active reservoir monitoring: 74th Annual International Meeting, SEG, Expanded Abstracts, 2263.

J. Cotton, E. Forgues, 2012, Dual-Depth Hydrophones for Ghost Reduction in 4D Land Monitoring: 82th Annual International Meeting, SEG, Expanded Abstracts number 667.

J. Cotton, E. Forgues and J.C. Hornman, 2012, Land Seismic Reservoir Monitoring: Where is the steam going? : 82th Annual International Meeting, SEG, Expanded Abstracts number 1539.

J.C. Hornman, J. Van Popta, C. Didraga, and H. Dijkerman, 2012, Continuous monitoring of thermal EOR at Schoonebeek for intelligent reservoir management: International Intelligent Energy Conference, SPE, 150215.